Polymer 51 (2010) 2000–2006

Contents lists available at ScienceDirect

Polymer

journal homepage: www.elsevier.com/locate/polymer

Formation of nanostructured composites with environmentally-dependent electrical properties based on poly(vinylidene fluoride)–polyaniline core–shell latex system

Gururaj M. Neelgund [a], Valery N. Bliznyuk [a,*], Alexander A. Pud [b], Kateryna Yu. Fatyeyeva [b], Erika Hrehorova [a], Margaret Joyce [a]

[a] Department of Paper Engineering, Chemical Engineering and Imaging, Western Michigan University, Kalamazoo, MI 49008, USA
[b] Institute of Bioorganic Chemistry and Petrochemistry of National Academy of Science of Ukraine, 50, Kharkivske Schose, 02160 Kyiv, Ukraine

ARTICLE INFO

Article history:
Received 21 December 2009
Received in revised form
16 February 2010
Accepted 21 February 2010
Available online 1 March 2010

Keywords:
Sensor
Poly(vinylidene fluoride)
Polyaniline

ABSTRACT

Submicron poly(vinylidene fluoride) (PVDF)/polyaniline (PANI) core–shell latex particles are synthesized and examined as an active component in a simple conductometric chemical sensor. The structure and physical properties of these particles and nanostructured composite PVDF–PANI polymer films built of them are characterized with transmission electron, atomic force, and helium ion microscopy techniques, differential scanning calorimetry, and conductivity measurements. The nanostructured composite films with conductivity of about 4×10^{-4} S/cm suitable for sensor applications are prepared by casting from the core–shell particles dispersions on glass substrates patterned with silver electrodes followed by annealing at 180 °C, i.e. above T_m of the PVDF component. Sensor properties of these films are tested by measuring current–voltage (I–V) characteristics in response to varying concentration of NH_3 or HCl vapors. The developed thin film sensor heterostructures with electrically conductive percolation network of PANI as an active component and employing the conductometric detection scheme show high sensitivity to both analytes. However, the polymer material is especially efficient for application to NH_3 sensing with the detection limit as low as 100 ppb, and good reproducible recovery behavior upon repeated exposure to NH_3 at ambient conditions.

1. Introduction

Intrinsically conducting polymers (ICPs) can be used as chemical sensor materials due to the fact that their conductivity and optical properties are very sensitive to their doping level, which in turn can be easily effected by different external chemical agents. [1,2] In fact conductivity of ICPs such as polyacetylene, polyparaphenylene vinylene, polypyrroles, polythiophenes etc. can be changed in a very broad range from semiconducting or even insulating properties (10^{-6}–10^{-10} S/cm) to highly conductive "quasi-metallic" state with the conductivity approaching that of copper ($\sim 10^4$ S/cm). This makes ICPs attractive materials for usage as active components of sensors to identify different chemical substances and, in some cases, even some physical factors [3,4]. In turn these changes are the basis of simple mechanisms of transduction of events, which include specific chemical and/or physical interactions of these polymers with effecting factors, into electric or optical signals [5].

Among ICPs polyaniline (PANI) has the best combination of sensor properties, stability, conductivity, cost, etc. [6]. The significant distinction of PANI from other ICPs is its ability to react, dependently on degree of doping, reversibly with basic or acidic environment. The PANI's response to the environment is not due to a variation of the redox-state, but originates from a variation of the degree of protonation of the polymer chains that results both in color (spectral) and conductivity changes of the material [3,7,8]. This mechanism is based on the simple reversible interaction of emeraldine salt or base forms of PANI with compounds having base or acid functions correspondingly. Such changes can be easily registered and processed by proper devices especially in case of nanostructured PANI materials, which show enhanced magnitude and response rate of these signals due to a high specific surface area and enhanced accessibility of their sensitive centers [9–11]. Naturally, the sensing response essentially depends also on the PANI material morphology [12], and on the degree of doping [13].

The above considerations put two mutually exclusive requirements to the design of advanced functional materials (both PANI

* Corresponding author. Tel.: +1 269 2763213.
E-mail address: valery.bliznyuk@wmich.edu (V.N. Bliznyuk).

0032-3861/$ – see front matter © 2010 Elsevier Ltd. All rights reserved.
doi:10.1016/j.polymer.2010.02.038

and other ICP based ones) for sensor applications: 1) enhancement of the proportion of functional groups located on the surface of the material and therefore readily available for specific interaction with an analyte; 2) the easiness of integration of a new material into existing microelectronics fabrication protocols. The first requirement can be satisfied in materials based on nanoparticles (like PANI nanotubes or nanofibers). However such materials have a drawback of more complex fabrication protocols and do not possess sufficient mechanical stability [14,15]. As an alternative, more robust and mechanically stable highly porous bulky materials can be used [16,17]. The latter are perfectly compatible with the existing traditional deposition and processing technologies but have generally longer sensor response time, reduced sensitivity and poorer reproducibility in comparison to the nanoparticles analogs. We have demonstrated in our paper how the above dilemma in application of the nanoparticles or highly porous bulky materials can be resolved in the framework of the approach using a system of submicron core–shell polymer particles. In the latter case the PANI functional sensing shell can be structured at the nanoscale through application of special polymerization approaches [18–20], while more bulky and heavy core insures mechanical stability of the material as the whole. Moreover the core itself might play an important special function in the system. For instance, it can introduce desirable physical properties like macroscopic polarization, optical transparency, mechanical toughness and thermal processability. This approach simultaneously dramatically reduces human health and environmental risks associated with formation of aero-sols in existing nanofabrication protocols [21,22].

In this connection, we directed our efforts on the investigation of possibility for creation of nanostructured electrically conductive composites based on recently developed poly(vinylidene fluoride)–PANI, doped with dodecylbenzenesulfonic acid, (PVDF–PANI–DBSA) submicron core–shell particles [23] PVDF as a core polymer material possesses simultaneously convenient range of melting transition temperature, good processability, chemical inertness against many organic solvents, acids and bases, and thermal stability of properties [24]. As an additional advantage, PVDF latex particles have higher density ($\rho = 1.78$ g/cm^3) in comparison to other common polymer latex materials (e.g. 1.05 g/cm^3 for polystyrene and 1.19 g/cm^3 for poly(methyl methacrylate)). The higher density of PVDF helps to minimize problems associated with the nanoparticle dust formation and possible risks of its inhalation during processing operations. In our research, we intended to study the morphology, electrical properties and their variation for the PVDF–PANI core–shell polymer system depending on the preparation conditions. We also wanted to make assessment of such nanostructured composite material as an active component for possible sensor applications. For this, NH_3 and HCl vapors as typical and practically important analytes, strongly affecting the electrical conductivity of PANI, were applied.

2. Experimental

2.1. Preparation of PVDF/PANI–DBSA core–shell particles

The core–shell particles were prepared through a procedure described elsewhere [23]. Specifically, aniline (Merck) was polymerized under the action of oxidant potassium persulfate ($K_2S_2O_8$) in a medium of PVDF 1000 Kynar latex (Arkema) in the presence of DBSA (Acros) at 10 °C for 5 h under stirring. The latex contains PVDF submicron particles with average diameter ~200 nm. DBSA functioned in this system as a surface active substance, a plasticizing agent and a dopant for the PANI component. The molar ratio of aniline: DBSA and aniline:$K_2S_2O_8$ were 1:1.5 and 1:1.25, respectively. The concentrations of the reagents allowed 4.8 wt.% PANI–DBSA loading in the hybrid particles. After the polymerization was completed, the disperse phase of PVDF/PANI–DBSA was rinsed with an excess of water, and finally dried under vacuum at 70 °C to a constant weight. The final PVDF/PANI–DBSA composite powder was used in further tests.

2.2. Deposition of the PVDF–PANI films

Nanostructured PVDF–PANI films were prepared via casting of the PVDF–PANI dispersions on glass slides with thermally evaporated silver electrode pattern. For this, a 4 wt.% dispersion of PVDF or PVDF–PANI latexes were prepared in chloroform (Aldrich) and then cast onto the glass surface. The solvent was allowed to evaporate at room temperature. After proper drying, the films were additionally annealed at temperature 180 °C for various periods of time (0–30 min) in a laboratory oven. The film thickness was measured from AFM as an elevation of the film surface over the glass substrate at places of artificially produced scratches. These measurements showed relatively uniform film thickness with a standard deviation of less than 15% of the mean value.

2.3. Electrical and sensor measurements

The electrical measurements were carried out with a Keithley 2400 multimeter in accordance to a procedure described elsewhere [24]. The prepared amperometric devices (i.e., glass slides with patterned silver electrodes and active polymer latex films deposited on top) were exposed to NH_3 and HCl vapors of variable concentrations in air and their electrical properties in terms of I–V characteristics were monitored in the voltage range −1 V to +1 V at room temperature in a specially designed test chamber of 1 L volume. During the sensing measurement, gas concentrations of the NH_3 or HCl analytes were altered by injecting the sample gas into the airtight testing chamber using a sample injector (syringe). The variation of current was simultaneously measured depending on the applied voltage and the analyte concentration. The variation of the current at a constant voltage was also monitored for several cases as a function of time and depending on the concentration of the NH_3 or HCl analyte to measure the rate and reproducibility of the sensing response. Raw current measurements were used for estimation of electrical conductivity for several samples using the equation: $\sigma = ID/U{\cdot}A = ID/U{\cdot}(W{\cdot}T)$; where σ is electrical conductivity, I is experimentally measured current under applied voltage U, D is the gap between planar electrodes, and A is the cross-sectional area of the sample (can be estimated as a product of the electrodes' width, W, and the film thickness, T) [24]. The electrodes for these measurements were fabricated by thermal evaporation of silver on cleaned glass slides in vacuum 10^{-5} torr. Typically they had the width W in the range of 5–15 mm and the gap $D = 200$ μm.

2.4. Structure and physical properties characterization

The size of the PVDF particles and uniformity of PANI coating on PVDF particles were investigated utilizing JEOL JEM-100CXII transmission electron microscope (TEM). The thermal behavior of the PVDF–PANI particles was characterized using Perkin–Elmer Pyris 1 DSC system in air with the heating rate of 20 °C/min. The morphological characterization of the films was conducted using an Autoprobe CP AFM equipment (ThermoMicroscopes Inc.), operated in a tapping mode with silicon nitride tips and ORION™ helium ion microscope (HIM) (Carl Zeiss SMT, Inc., Peabody, MA).

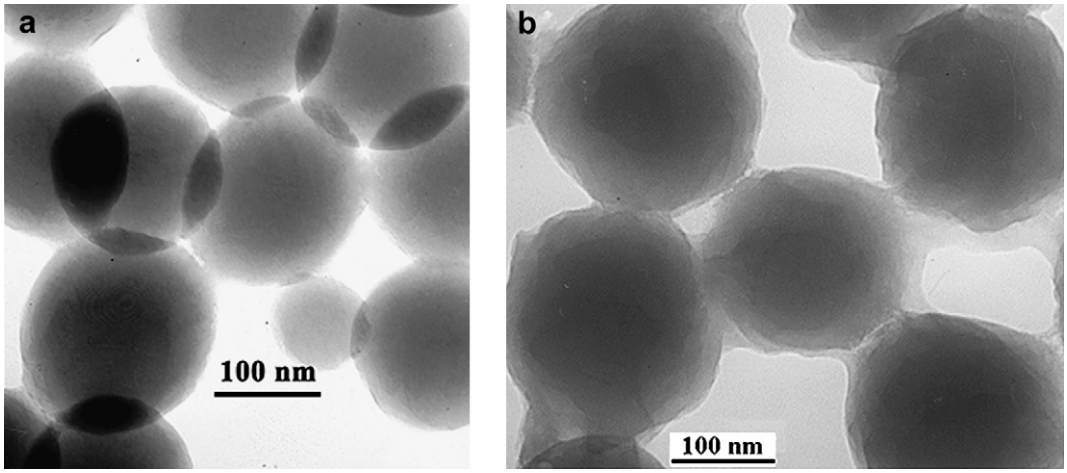

Fig. 1. TEM images of (a) PVDF latex particles and (b) PVDF–PANI core–shell latex particles.

3. Results and discussion

Fig. 1 provides the transmission electron microscopy (TEM) images of PVDF latex particles before and after modification with PANI. Unmodified PVDF particles were found to possess an average size of 200 nm and a uniform size distribution (Fig. 1(a)). Modified latex particles (PVDF–PANI core–shell system) have larger diameter (about 220 nm) as can be seen from their TEM image (Fig. 1(b)). Presence of the PANI shell is displayed here as a semi-transparent quite uniform layer, which surrounds more dense and smooth PVDF particles. It should be mentioned here that formation of PANI shells at the surface of various particles due to aniline polymerization in water dispersions is the well known signature of the PANI polymerization process [25,26].

The thermal behavior of the unmodified and PANI modified PVDF particles was addressed with differential scanning calorimetry (DSC) and the resulting thermograms are presented in Fig. 2(a) and (b). The melting transition temperature (T_m) of PVDF latex particles can be seen as a sharp endothermic peak in the heating portion of the thermograms accompanied with well-pronounced reversed peaks of crystallization in the cooling portions of the curves. Similar behavior has been observed for PVDF/PANI–DBSA core–shell particles. One can see that the polymerization of aniline and creation of the PANI shell on top of the PVDF core has almost no effect on the crystalline properties of the latter. Specifically, PANI–DBSA modified PVDF core–shell particles possess T_m which is just 0.8° lower than that of pristine PVDF particles (Fig. 2(a) and (b)). The effect can be probably due to a plasticizing effect of a small quantity of DBSA. PVDF and PVDF/PANI–DBSA latex systems are however significantly different in sense of their crystallization temperatures when cooled from the melt state. The latter effect can be ascribed to the presence of the PANI–DBSA shells acting as seeding centers for heterogeneous nucleation and promoting higher crystallization temperature in the case of PVDF–PANI–DBSA system in comparison to pure PVDF. Several minor peaks seen in the DSC curves belong to impurities, have not been reproducible from scan to scan and therefore are not interpreted.

With the known geometrical parameters of the film (i.e., film thickness, width of the silver electrodes and the gap between them) it was possible to estimate the electrical conductivity from registered current-voltage characteristics (I–V curves) [24]. The film thickness was in the range of 300–800 nm (as measured from

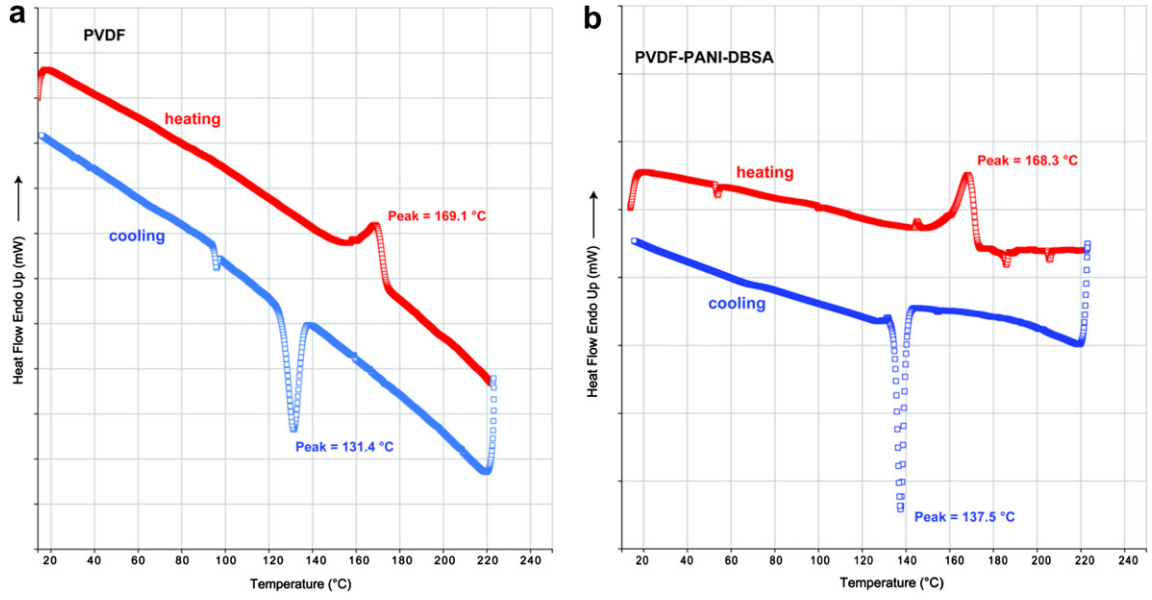

Fig. 2. DSC thermograms of (a) PVDF latex particles and (b) PVDF–PANI core–shell latex particles.

AFM scans) that corresponded roughly to 2–5 layers of the latex particles. To ensure formation of a robust PVDF–PANI composite, these films were subjected to annealing at 180 °C (i.e. above T_m of the PVDF core component). The initial electrical conductivity of as prepared PANI–PVDF film at room temperature was relatively poor (3×10^{-5} S/cm). However, during annealing for 3 min at 180 °C, the film conductivity first increased sharply to 4×10^{-4} S/cm followed by a gradual decrease to some intermediate value ($\sim 1.5 \times 10^{-4}$ S/cm). Variation of the relative conductivity can be represented in terms of changes of the slope in *I–V* curves. Such curves recorded at room temperature after different times of annealing at 180 °C are depicted in Fig. 3. As can be seen the maximum in conductivity could be achieved after approximately 3 min of such heat treatment. This figure gives an example of current variation measured for the same sample. The experimental values of the current (but not of the conductivity) varied significantly (up to 100 times) from sample to sample depending on the geometrical parameters of the electrode pattern, the film thickness and individual variation of the morphology during annealing. Nevertheless, Fig. 3 shows correctly the general trend of current variation with the annealing time and is representative for all tested devices. We can speculate that the observed increase in conductivity is a result of some morphological changes in the film due to application of the elevated temperature. The simplest explanation is that the annealing above the T_m of PVDF facilitates the mobility and inter-diffusion of the PVDF chains resulting in a higher compactness of their structural organization. In turn this brings better electrical contact between the neighboring conducting PVDF–PANI–DBSA particles, fills the voids, and creates a conductive percolation network with increased mobility of charge carriers. These results are in agreement with earlier reports [27,28]. The cause for the decrease of electrical conductivity for longer annealing times may be associated with some thermal aging of the PVDF–PANI particles, which is probably enhanced at elevated temperatures. Previous studies demonstrated that the chemical structure and electrical conductivity of conductive polymer materials could be seriously influenced by the oxidation reactions when exposed to air at elevated temperatures [27,29,30]. Several thermally stimulated chemical processes (oxidation, hydrolysis, or crosslinking) might be expected in the PVDF–PANI system. The oxidation effect could be probably diminished if annealing is performed under vacuum or under inert atmosphere conditions. Additionally, the thermal dissociation of PANI–DBSA salt might result in the redistribution of the DBSA dopant within the polymer film with the possibility of DBSA migration into PVDF melt and so in the reduction of the PANI component doping level. Such scenario is

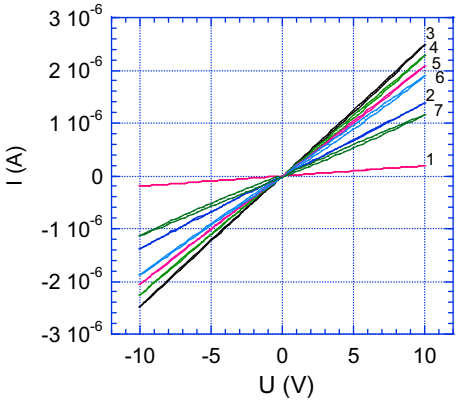

Fig. 3. Change in *I–V* characteristics for dispersion cast PVDF–PANI film (300 nm thickness) annealed at 180 °C for different periods of time: (1) as prepared; (2) 1 min; (3) 3 min; (4) 4 min; (5) 5 min; (6) 10 min; and (7) 20 min.

supported by our and other groups DSC experiments on PANI–DBSA systems [24,31]. The initial thermal run is characterized with a thermal transition at around 130 °C (which can be assigned to the glass transition [31]) disappearing after several thermal scans. These observations demonstrate the redistribution of the dopant, which acts simultaneously as a PANI plastisizer, leading to an increase of the PANI's T_g and to a severe reduction of the conductivity in the system. Therefore, a 3 min annealing time was chosen as an optimum duration to achieve the highest conductivity in the PVDF–PANI latex system, and the same annealing procedure was used in all further experiments.

The changes of the films morphology were studied by AFM and HIM techniques. The PVDF–PANI particles deposited on glass substrate were basically spherical before annealing, as seen in Fig. 4 (a) and (c). These spherical particles gradually melt and become flattened when annealed at 180 °C (Fig. 4(b) and (d)). As can be seen, the film is still highly porous after the annealing procedure, although, the voids inside the film gradually disappear. The size of the pores is corresponding roughly to the size of latex particles. As the adjacent particles deform under the annealing treatment (sintering) their contact surface area increases, which results also in an enhancement of the conductivity of the film. After prolonged annealing (20 min or more), phase separation between PVDF and PANI–DBSA components and dewetting of the polymer film from the substrate has been observed. Visually, the color of the PVDF/PANI–DBSA film changed from beautiful green to a "dull green" after annealing for 20 min which was also in tune with possible chemical degradation of PANI under exposure to oxygen. Finally, due to the slow degradation of the PVDF/PANI–DBSA film its electrical conductivity was also significantly reduced. All changes in the morphology occurring during annealing are schematically represented in Fig. 5. This cartoon shows that core–shell particles preserve their spherical shape in the original (as cast) film (Fig. 5a) but are melted and sintered into a porous monolithic film with a continuous PANI phase and domains of crystalline PVDF after 3 min of high temperature annealing (Fig. 5b). Longer thermal treatment causes macro-phase separation and dewetting of the components from the glass substrate due to their immiscibility and different affinity to silica substrate (Fig. 5c).

Fig. 6 shows how *I–V* characteristics of the PVDF–PANI–DBSA film are affected by adding 0.1 ppm NH_3 to the air environment. The current was measured during the sweep of voltage in the range of −1 V to +1 V upon injection of a desirable amount of ammonia gas into the sensing chamber with a syringe. All *I–V* curves show a linear (Ohmic) behavior. However the exposure to ammonia reduces gradually the current passing through the film giving evidence of variation of the polymer film conductivity due to its contact with the environment. The interaction of NH_3 with such the nanocomposite films is well confirmed with Fig. 7a, which presents typical examples of kinetic profiles of changes of responses of such sensor films when in contact with two low NH_3 concentrations. The value of the sensor response S is determined as a relative change of the polymer sample current ($I_0 - I$) related to the initial current (I_0): $S = \Delta I/I_0 \times 100\%$. As one can see the measured electrical current decreased by about 16% for 1 min independently on what ammonia concentration (in the range of 0.1–1 ppm) has been applied. The real registered difference ($\sim$8%) in the responses (S) of the composite film under action of 0.1 ppm and 1 ppm ammonia concentrations was observed only after 3 min of the exposure (Fig. 7a). Then the kinetic profiles of the sensing process tend to saturation at $\sim$ 80% decrease of the initial signal for 60 min but with the rate depending on the ammonia concentration (Fig. 7) and do not get complete signal damping even for 150 min. The nature of this sample interaction with NH_3 is obviously the same as for doped PANI [7]. Specifically, when NH_3 vapors interact with

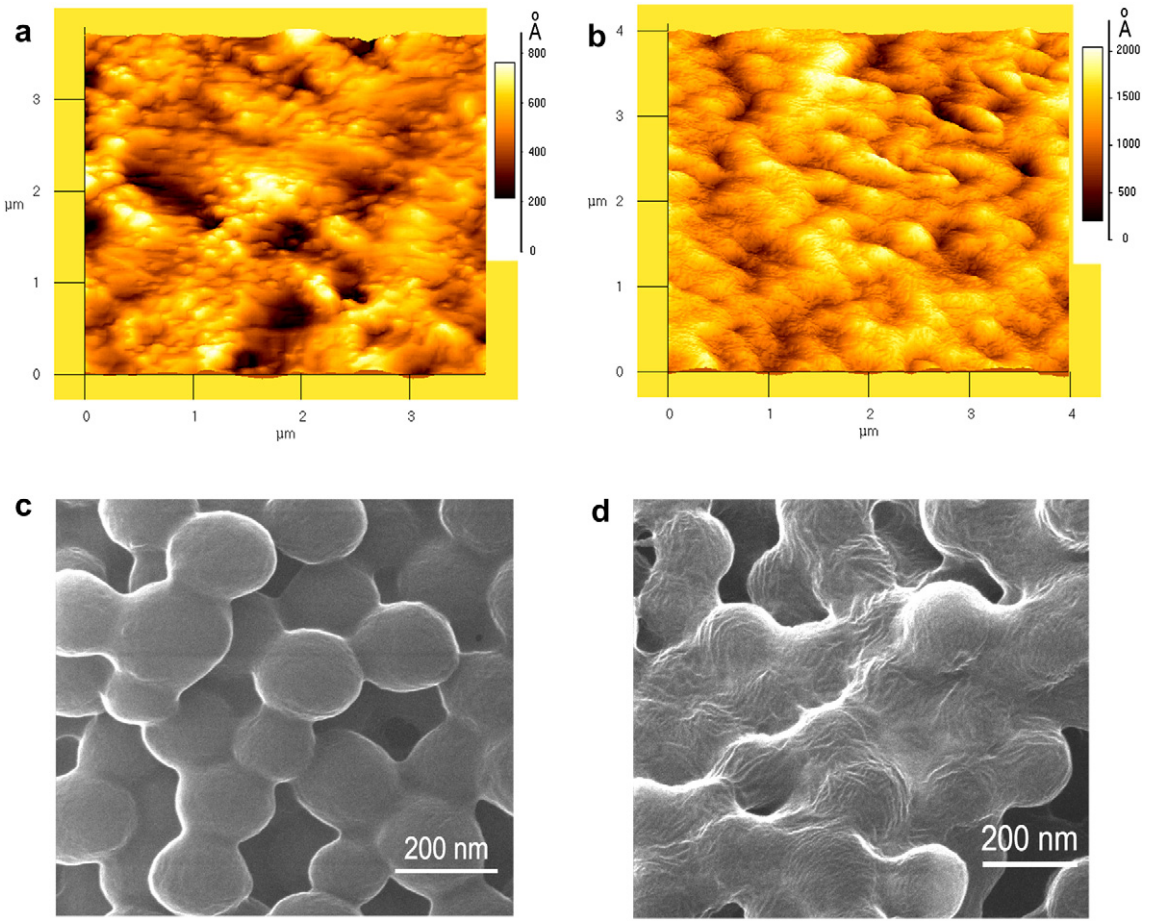

Fig. 4. AFM tapping mode (a, b) and ORION™ helium ion microscopy (c, d) images of as prepared PVDF–PANI film (a and c), and PVDF–PANI film annealed at 180 °C for 3 min (b and d).

PVDF/PANI–DBSA film, the NH_3 molecules compete with PANI for the acid dopant (DBSA). In a solid phase they pull aside protons H^+ from the doped PANI due to their stronger basicity. The process can be understood as just a simple competition for DBSA between a weak base (PANI) and a stronger base (NH_3). As a result, the quantity of positive charges at PANI molecules decreases leading to a significant drop of the electrical conductivity in the system. However, in the nanocomposite case the rate of this process should obviously depend not only on NH_3 concentration but also on accessibility of PANI sensing sites, which in turn is determined by the polymer film's porosity and the thickness of the PANI shell.

Although the found behavior of the nanocomposite is typical for PANI-based sensor materials [7,9], its simple and easy *in situ* registration scheme under action of low ammonia concentrations

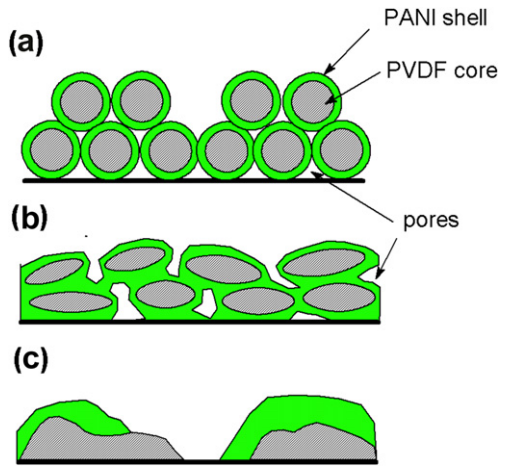

Fig. 5. Schematic representation of morphological changes which happen on the surface of PVDF–PANI films at different stages of the annealing (see more explanations in text).

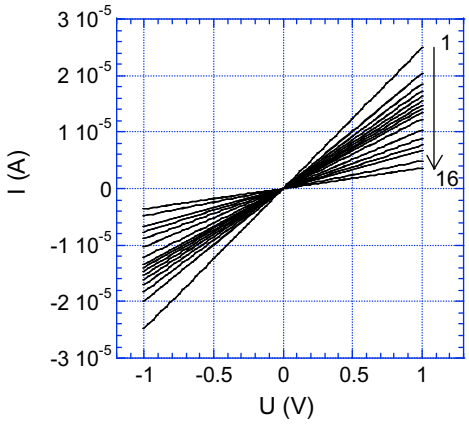

Fig. 6. *I–V* characteristics for PVDF–PANI film depending on the ammonia exposure: (1) a pristine film cast from chloroform dispersion and then thermally annealed at 180 °C for 3 min (film thickness 600 nm). The same film after different time of the exposure to 0.1 ppm NH_3: (2) 1 min; (3) 3 min; (4) 5 min; (5) 7 min; (6) 9 min; (7) 11 min; (8) 13 min; (9) 15 min; (10) 20 min; (11) 30 min; (12) 40 min; (13) 50 min; (14) 60 min; (15) 90 min; and (16) 120 min.

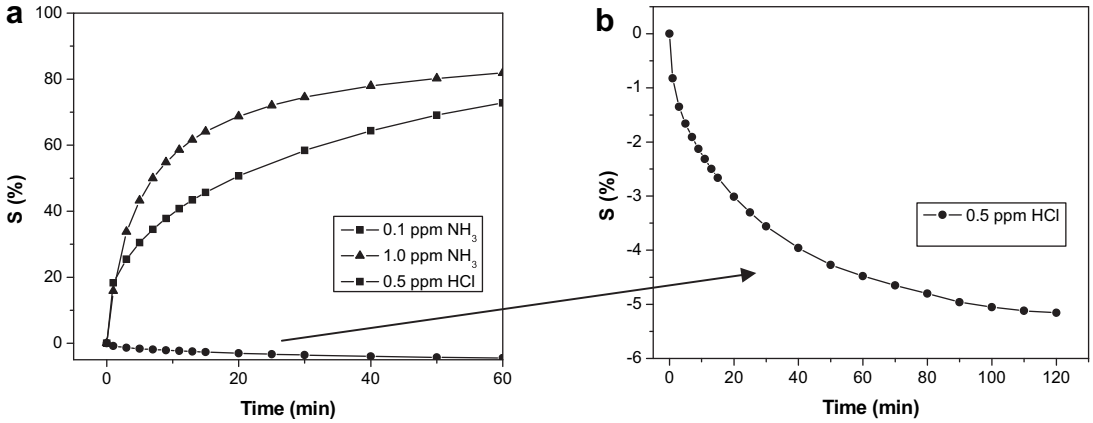

Fig. 7. Kinetic profiles of sensor responses of PVDF–PANI film exposed to NH_3 (a) and HCl (b) vapors.

(0.1–1 ppm) suggests its good prospects as an active component for chemical sensors. However, this application will become possible only under conditions of an additional improvement of the material's response. The last issue is crucial because for the practically meaningful time of the material sensor response (<1 min) the developed nanostructured PVDF–PANI–DBSA film does not allow to differentiate 0.1 ppm and 1 ppm ammonia concentrations.

Interestingly enough, the PVDF–PANI–DBSA films show increase of their conductivity when being exposed to low concentration of HCl vapors despite their already doped state. Fig. 7b shows the sensor response S dependence on time of the exposure for 0.5 ppm HCl concentration as an example. The observed phenomenon is probably due to the fact that HCl causes additional doping of free imine sites present in the PANI chains due to both incomplete doping after washing of the freshly synthesized sample and to the described above procedure of pre-treatment annealing of the film. This additional doping with HCl in turn stimulates the appearance of new polarons and bipolarons in the system and results in an enhancement in conductivity. However, because PANI chains are already doped with DBSA moieties (the initial current measured in air I_0 is already high) this does not lead to a significant enhancement of the conductivity level. Therefore, the response of the PVDF–PANI–DBSA sensor to HCl is not as substantial and is not so fast when compared to NH_3. A special de-doping procedure may be required for the enhancement of the system response to HCl.

PVDF–PANI films were also exposed alternately to NH_3 vapors (0.1 ppm) and to air at room temperature for repeated cycles to measure the reproducibility of the sensor response. A similar procedure was followed with application of 0.1–5 ppm concentration of HCl vapors. Good reproducibility was observed upon repeated exposure to both analytes.

4. Conclusions

The latex films consisting of tightly bound PVDF/PANI–DBSA core–shell submicron particles with PANI shells of up to 10 nm thickness demonstrate high sensitivity to gaseous ammonia with a detection limit of about 0.1 ppm or less. Our results testify that this composite material has a good potential to be used as a sensing material to detect ammonia but will require further enhancement of the response time for practical application. Interestingly, due to an incomplete doping of the polymer chains, this material is also sensitive to gaseous HCl but in a narrower concentration range. This fact gives good prospects that upon complete de-doping of PVDF/PANI–DBSA (i.e., complete removing of the DBSA molecules), the material will become also highly sensitive to HCl in a wide range of concentrations. In accordance with the known results for nanostructured PANI-based systems [7–10], the main reasons of such high sensitivity of the system should be the nanoscale thickness of the active PANI shells and high porosity of the sensing material. The latter is due to the fact that the polymer film is composed of a large quantity of submicron PVDF/PANI–DBSA core–shell particles. Using short-time annealing, above the melting point of the PVDF matrix, we could optimize the structure and conductivity properties of the material to achieve a better sensor response. It has been demonstrated that a short-time annealing treatment at temperature exceeding T_m of the PVDF can be used as an effective instrument to tune conductivity of nanostructured PANI containing composite materials and, respectively, to tune their sensor response. From practical viewpoint this property allows preparing stable and mechanically strong PVDF/PANI–DBSA films with excellent sensing properties.

Acknowledgements

The authors are grateful to Dr. Larry Scipioni and Mr. Chuong Huynh, Carl Zeiss SMT, Inc., USA for their helium ion microscopy study of the samples' morphology.

References

[1] Hakansson E, Lin T, Wang H, Kaynak A. Synth Met 2006;156:1194.
[2] Curran SA, Zhang D, Dundigal S, Blau W. J Phys Chem B 2006;110:3924.
[3] Bai H, Shi G. Sensors 2007;7:267.
[4] Jang J. Adv Polym Sci 2006;199:189.
[5] Li G, Josowicz M, Janata J, Semancik S. Appl Phys Lett 2004;85:1187.
[6] Cao Y, Smith P, Heeger AJ. Synth Met 1992;48:91.
[7] Nicolas-Debarnot D, Poncin-Epaillard F. Anal Chim Acta 2003;475:1.
[8] Pron A, Rannou P. Prog Polym Sci 2002;27:135.
[9] Huang X, Choi Y. Sens Actuators B 2007;122:659.
[10] Virji S, Huang J, Kaner RB, Weiller BH. Nano Lett 2004;4:491.
[11] Huang J, Virji S, Weiller BH, Kaner RB. J Am Chem Soc 2003;125:314.
[12] Li G, Martinez C, Janata J, Smith A, Josowicz M, Semancik S. Electrochem Solid State Lett 2004;7:H44.
[13] Janata J, Josowicz M. Nat Mater 2003;2:19.
[14] Pud A, Ogurtsov A, Korzhenko A, Shapoval G. Prog Polym Sci 2003;28:1701.
[15] Malinauskas A. Polymer 2001;42:3957.
[16] Jin Z, Su Y, Duan Y. Sens Actuators B 2001;72:75.
[17] Yang J, Martin DC. Sens Actuators B 2004;101:133.
[18] Vincent B. Polym Adv Technol 1995;6:356.
[19] Tai H, Jiang Y, Xie G, Yu J, Chen X. Sens Actuators B 2007;125:644.
[20] Barthet C, Armes SP, Lascelles SF, Luk SY, Stanly HME. Langmuir 1998;14:2032.
[21] Wardak A, Gorman ME, Swami N, Deshpande S. J Ind Ecology 2008;12:435.
[22] Hutchison JE. ACS Nano 2008;2:395.
[23] Korzhenko A, Pud A, Shapoval, G. Patent US 7, 211, 202 B2, 2007.
[24] Bliznyuk VN, Baig A, Singamaneni S, Pud AA, Fatyeyeva KY, Shapoval GS. Polymer 2005;46:11728.

[25] Pud AA, Noskov Yu V, Kassiba A, Fatyeyeva KYu, Ogurtsov NA, Makowska-Janusik M, et al. J Phys Chem B 2007;111:2174.
[26] Stejskal J, Quadrat O, Sapurina I, Zemek J, Drelinkiewicz A, Hasik M, et al. Eur Polym J 2002;38:631.
[27] Liau W, Sun Y, Yang L, Wang L, Chiu W, Hsieh K, et al. J Appl Polym Sci 2006;102:5406.
[28] Huijs FM, Vercauteren FF, Hadziioannou G. Synth Met 2002;125:395.
[29] Stejskal J, Omastova M, Fedorova S, Prokeš J, Trchova M. Polymer 2003;44:1353.
[30] Prokeš J, Trchova M, Hlavata D, Stejskal J. Polym Degrad Stab 2002;78:393.
[31] Hoa ND, Quy NV, Cho Y, Kim D. Sens Actuators B 2007;127:447.